Journal of Process Control 22 (2012) 1468–1477

Contents lists available at SciVerse ScienceDirect

Journal of Process Control

journal homepage: www.elsevier.com/locate/jprocont

Robust nonlinear internal model control of stable Wiener systems

Kwang-Ki Kevin Kim[a,b], Ernesto Ríos-Patrón[c], Richard D. Braatz[a,b,*]

[a] Massachusetts Institute of Technology, Room 66-372, Cambridge, MA, USA
[b] University of Illinois at Urbana-Champaign, Urbana, IL, USA
[c] Petróleos Mexicanos and Facultad de Quimica, UNAM, Mexico City, Mexico

ARTICLE INFO

Article history:
Received 20 June 2011
Received in revised form 4 December 2011
Accepted 24 January 2012
Available online 27 March 2012

Keywords:
Nonlinear control
Robust control
Wiener systems
Internal model control
Linear matrix inequalities

ABSTRACT

Many process systems can be modeled as a stable Wiener system, which is a stable linear system followed by a static nonlinearity. A nonlinear control design procedure is presented that provides robustness to uncertainties while being applicable to systems with unstable zero dynamics, unmeasured states, disturbances, and measurement noise. The design procedure combines nonlinear internal model control with linear matrix inequality feasibility or optimization problems, such that all robust stability and performance criteria are computable in polynomial-time using readily available software. Application to a pH neutralization case study demonstrates the importance of taking uncertainty into account during the design of controllers for Wiener systems. The approach is generalizable to Hammerstein and sandwich systems, whether well- or poorly conditioned, and to systems with actuator constraints.

1. Introduction

A Wiener model consists of a linear dynamic system G followed by a static nonlinear operator Γ (see Fig. 1). Many process systems have been described by Wiener models including distillation columns [1], heat exchangers [1], pH neutralization [2], packed bed reactors [3], and plasma reactors [4,5]. Various control strategies have been developed for Wiener systems, including adaptive control [6], linearizing feedforward-feedback control [7], and model predictive control [8,9] strategies, many of which have been evaluated by application to pH neutralization processes.

The static nonlinearity in a Wiener model for a practical application is always uncertain, and most existing methods for the control of Wiener systems ignore this uncertainty. As will be demonstrated in a case study later in this paper, the uncertainty in the nonlinearity can have major effects on the closed-loop stability and performance. While robust optimal controllers for Wiener systems have been designed by formulating the optimal control problem in terms of bilinear matrix inequalities (BMIs) [4,5], a drawback of such an approach is that optimization over BMIs is an NP-hard problem [10]. This paper proposes an approach that only involves convex programs that can be solved using off-the-shelf software in polynomial-time. The proposed approach is applicable to stable Wiener systems with unstable zero dynamics, unmeasured states, disturbances, and measurement noise. A novel aspect of the approach is that various characteristics of the nonlinearities can be taken explicitly into account in the closed-loop stability and performance analyses. The approach is applied to a case study involving the control of pH in which the Wiener model is identified from experimental data. The control of pH is an important industrial problem that has been extensively studied [11–15].

2. Theory

2.1. Standard nonlinear operator form

The proposed approach employs the standard nonlinear operator form (SNOF) in Fig. 2, which has its roots in the 1940s Russian control literature [16–18]. The SNOF consists of a linear system with a static nonlinear operator in feedback, where the static nonlinearities of the operator can be further restricted to be diagonal, monotonic, and locally slope-restricted. Nearly any arbitrary nonlinear system (including unstable zero dynamics, chaotic, and quasi-periodic behavior) can be approximated with arbitrary accuracy by a model in standard nonlinear operator form [19]. Furthermore, all dynamic artificial neural networks can be transformed into the SNOF, so that any of the software packages available for fitting DANNs to experimental data[1] produces models that can be written in SNOF. The static, monotonic, and locally slope-restricted nature of the nonlinearities can be exploited to produce

* Corresponding author.
E-mail address: braatz@mit.edu (R.D. Braatz).

[1] The Matlab neural network toolbox

0959-1524/$ – see front matter
doi:10.1016/j.jprocont.2012.01.019

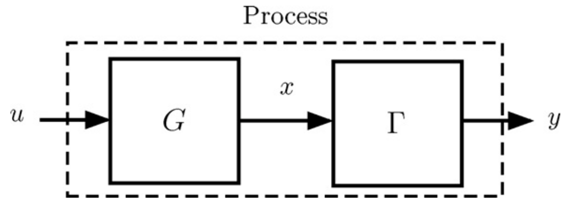

Fig. 1. Wiener model structure where G is linear time-invariant and Γ is a static nonlinearity.

polynomial-time tools to analyze the stability and performance of these systems (e.g. see [20,21] and references cited therein). The analysis tools can be written in terms of linear matrix inequalities (LMIs) [22], which are computable using available software (e.g. [23,24]), much of which can be run in Matlab. The proposed nonlinear control design stategy, described below, weds the above analysis tools with internal model control.

2.2. Nonlinear internal model control strategy

As is standard in inversion-based control strategies for the control of Wiener systems (e.g. see [25] and citations therein), the control structure has the form in Fig. 3, where Γ_2 is selected to be either the identity or the inverse of the process nonlinearity Γ_1, depending on whether the overall controller is desired to be linear or nonlinear. For nonlinear Γ_2, the controller in Fig. 3 has the Hammerstein structure, in which a dynamic linear controller K_L is augmented with the inverse of the nonlinear operator combined with the identified parameters of the process W_1 and W_2.

The remaining task is to determine the linear time-invariant controller K_L based on some closed-loop criteria. For example, an example of an $\mathcal{L}_2$-optimal control problem would be to determine the K_L that minimizes a weighted combination of the worst-case effects of the disturbance d and noise n on the output z:

$$\text{Problem}: \quad \inf_{K_L} \ \alpha\left(\sup_{\|d\|_2\le 1}\|z\|_2\right) + (1-\alpha)\left(\sup_{\|n\|_2\le 1}\|z\|_2\right) \quad (1)$$
$$\text{s.t.} \quad \text{the closed-loop system in Fig. 3 is stable,}$$

where the weight $\alpha \in [0, 1]$. For a linear time-invariant process ($\Gamma_1 = \mathbf{I}$), it is well known that the above optimal control problem is equivalent to a weighted $\mathcal{H}_\infty$-control objective, $\|w_u S + w_p T\|_\infty$, where S is the sensitivity function that maps the output disturbance d to the controlled output z, T is the complementary sensitivity function that maps the measurement noise n to z, and w_u and w_p are weights that define the tradeoff between disturbance suppression and insensitivity to measurement noise (e.g. [26,27]).

While there are several approaches available for solving $\mathcal{L}_2$-optimal control problems for linear time-invariant systems, solving such problems for nonlinear systems is much more challenging [28] and would require extensive software generation, even in the case where there is no uncertainty in the system. The nonlinearity Γ has associated uncertainty, so that the nonlinear inversion introduces nonlinear uncertainty into the closed-loop system. Rigorously taking that uncertainty into account while solving (1) results in a nonconvex optimization over bilinear matrix inequality constraints [4,5]. It is straightforward to show that optimizations over bilinear matrix inequality constraints are NP-hard,[2] either by reduction to the knapsack problem [10] or to an indefinite quadratic program [29]. An alternative approach is to parameterize K_L in Fig. 3 in terms of the well-known Youla parameterization (e.g. [26,27]), $K_L = Q/(1 - P_L Q)$, where the stable transfer function Q provides degrees of freedom for controller design. The engineer can parameterize Q in any way that maintains stability, and then tune the control parameters to optimize the objective (1).

Internal model control (IMC) restricts the degrees of freedom in Q so that the control tuning parameters are few and have a direct relationship to setpoint tracking response, disturbance suppression, insensitivity to measurement noise, and robustness to model uncertainties (e.g. [26,30]). The form for Q is selected as a low-pass filter F in series with the inverse of a minimum-phase approximation of the linear model of the stable process being controlled. For the notation used here, $Q = P_{L,\mathrm{m}}^{-1}$, where $P_{L,\mathrm{m}}$ is the minimum-phase approximation of the stable transfer function P_L.

Instead of directly solving an optimization such as (1) for the control tuning parameters, a common alternative is to tune the controller as fast as possible while satisfying all of the control objectives, such as guaranteed closed-loop stability with respect to all uncertainties with a prescribed set, effectiveness at disturbance suppression, or insensitivity to measurement noise (e.g. [31]). This approach avoids having to explicitly define a performance weight, and avoids having to balance the weights with respect to each other.

The above approaches apply to both continuous- or discrete-time systems; for brevity only the discrete-time equations will be presented below. To parametrize the controller, consider the low-pass filter

$$F(z) = \frac{1}{(\lambda((z-1)/(z+1))+1)^m}\mathbf{I} \quad (2)$$

where λ specifies the response speed of the low-pass filter and m is an integer that defines the order of the transfer function. This form for F is obtained from Tustin's discretization [32] of the low-pass filter $F(s) = \frac{1}{(\lambda s+1)^m}$ in the Laplace domain. The order of the low-pass filter is fixed and the control tuning parameter is the IMC filter time constant $\lambda > 0$. If needed, this filter form can be generalized to include numerator dynamics or different time constants in each diagonal element [26,33,34].

The closed-loop system in Fig. 3 can be rearranged into the SNOF in Fig. 2 by using block-diagram algebra as described in standard textbooks [26,31] or by using the *sysic* program in the Matlab Robust Control Toolbox. The next section presents methods to quantify robust stability and performance criteria for the closed-loop system in terms of linear matrix inequalities, which can be computed using off-the-shelf software that have Matlab interfaces (e.g. [23]). These quantifications can be inserted into an optimization formulation for λ using a weighted control objective such as (1) or can be used to determine the minimum value for λ that satisfies all of the robust stability and performance criteria.

Remark 1. The authors of [35] proposed an augmentation of the nonlinear controller with a linear filter, in which the model inverse was constructed using numerical procedures based on the contraction mapping principle and Newton's method. The same nonlinear IMC structure was later used [36], in which the model inverse was determined using differential geometry. The nonlinear control structure in Section 2.2 is very similar to those used in these and other past publications. As described in the next section, the proposed design method will differ from past works by rigorously taking uncertainties associated with nonlinear inversion into account.

3. Theory and methods: stability and performance criteria

3.1. Stability analysis

This section describes a necessary condition and sufficient conditions for the analysis of stability of a system in SNOF. To simplify

[2] Except for very specialized matrix structures

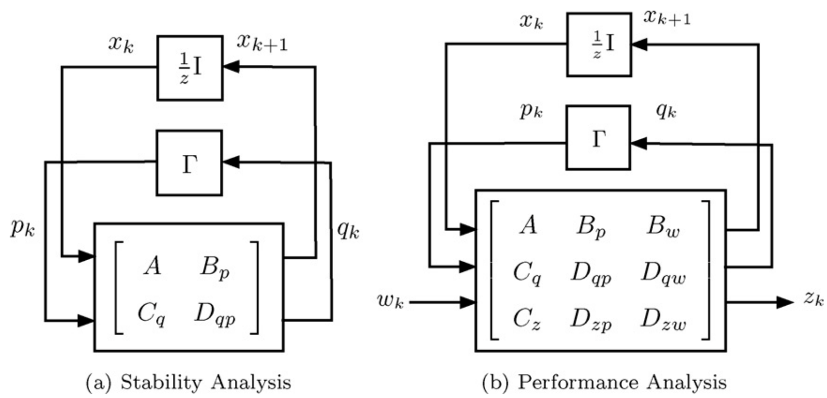

Fig. 2. Standard nonlinear operator form for discrete-time systems. The structure for continuous-time systems is obtained by replacing z with s, replacing x_{k+1} with dx/dt, and redefining the other variables to be continuous-time.

the notation, (B, C, D) is used as a shorthand notation for (B_p, C_q, D_{qp}).

The following necessary condition for stability of an SNOF is obtained from linearization of a nonlinear process model [37].

Theorem 1 (Necessary stability condition). *Consider a nonlinear system in SNOF as shown in Fig. 2(a):*

$$\begin{aligned} x_{k+1} &= Ax_k + Bp_k \\ q_k &= Cx_k + Dp_k \\ p_k &= \Gamma(q_k) \end{aligned} \tag{3}$$

where $x \in \mathbb{R}^n$, $p \in \mathbb{R}^h$, $q \in \mathbb{R}^h$, $A \in \mathbb{R}^{n\times n}$, $B \in \mathbb{R}^{n\times h}$, $C \in \mathbb{R}^{h\times n}$, $D \in \mathbb{R}^{h\times h}$, Γ is a diagonal nonlinear operator, n is the number of states, and h is the input-output dimension of Γ. A necessary condition for asymptotic stability of the steady-state x_{ss} is that the eigenvalues of the matrix

$$A_L(x_{ss}) \triangleq A + B\left(I - \left.\frac{\partial\Gamma}{\partial q}\right|_{ss} D\right)^{-1} \left.\frac{\partial\Gamma}{\partial q}\right|_{ss} C, \tag{4}$$

all have magnitude less than or equal to one, i.e., $\rho(A_L(x_{ss})) \le 1$ where $\rho(\cdot)$ denotes the spectral radius of a matrix.

The term $(\partial\Gamma/\partial q)\big|_{ss}$ is the Jacobian of Γ evaluated at the steady-state value for the state. For a diagonal $\Gamma =: \mathrm{diag}\{\gamma_i\}$, this Jacobian has a rather simple form, $(\partial\Gamma/\partial q)\big|_{ss} = \mathrm{diag}\{(\partial\gamma_i/\partial q_i)\big|_{x=x_{ss}}\}$.

Any of the sufficient conditions for analyzing the stability of systems in SNOF using linear matrix inequalities (e.g. see [22,38,39] and citations therein) can be applied to this approach. Which stability condition to apply depends on the assumptions made on the nonlinearities concerning the matrix structure (e.g. full-block, block-diagonal, or diagonal) and the extent of time variation (e.g. arbitrarily fast time-varying, arbitrarily slow time-varying, static). Which condition to use depends on the nature of the specific problem. For example, if the assumption that the process nonlinearity is static was only an approximation during the identification of the Wiener model, then a stability condition can be selected that allows the uncertainty in the nonlinear to be dynamic. If the nonlinearity in the Wiener model is multivariable, then a full-block uncertainty structure should be used. If the nonlinearities in the Wiener model are distinct and isolated, then a diagonal uncertainty structure should be used to reduce conservatism. Few of the published conditions, however, take into account the static, monotonic, and slope-restricted nature of most nonlinearities and such conditions that have been derived either require restrictive assumptions (see [20,21] for details). The following sufficient condition, which is computable for large-scale systems while taking into account these characteristics of nonlinearities, will be applied in the pH control case study.

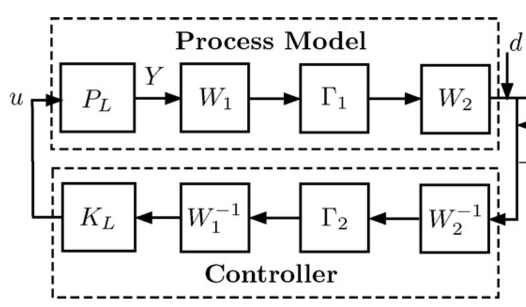

Fig. 3. Block diagram for the nonlinear closed-loop system, with output z, disturbance d, and noise n. The linear time-invariant and nonlinear static monotonic operators of the process are P_L (assumed to be stable) and Γ_1, respectively. The linear and nonlinear internal model controllers have $\Gamma_2 = 1$ and $\Gamma_2 \approx \Gamma_1^{-1}$, respectively.

Theorem 2 (Sufficient stability condition). [3] *Consider a system described in Fig. 2(a) with*

$$\begin{aligned} x_{k+1} &= Ax_k + Bp_k \\ q_k &= Cx_k + Dp_k, \end{aligned} \tag{5}$$

and $p_k = \Gamma(q_k)$ subject to the sector-bounded and slope-restricted conditions

$$\gamma_i(q_{k,i})[\gamma_i(q_{k,i}) - \xi_i q_{k,i}] \le 0, \quad \forall q_{k,i} \in \mathbb{R}, i = 1, \ldots, h \tag{6}$$

and

$$0 \le \frac{\gamma_i(q_{k+1,i}) - \gamma_i(q_{k,i})}{q_{k+1,i} - q_{k,i}} \le \mu_i, \quad \forall q_{k,i} \in \mathbb{R}, i = 1, \ldots, h \tag{7}$$

where ξ_i and μ_i is the maximum sector bound and slope of the ith nonlinearity, respectively. A sufficient condition for global asymptotic stability is the existence of a positive-semidefinite matrix $P = P^T$ with a positive-definite submatrix $P_{11} = P_{11}^T$ and diagonal positive-semidefinite matrices Q, $\tilde{Q}$, T, $\tilde{T}$, $N \in \mathbb{R}^{n_q\times n_q}$ such that the LMI

$$G \triangleq A_a^T P A_a - E_a^T P E_a + U_1 + U_2 - S_1 - S_2 - S_3 < 0 \tag{8}$$

holds, where the matrices A_a, E_a, U_1, U_2, S_1, S_2, and S_3 are defined in Appendices C and D.

[3] A preliminary version of this theorem was presented at the 2011 IEEE Multiconference on Systems and Control [20].

Although stated as a stability condition, Theorem 2 is also a robust stability condition, in that the existence of a feasible solution to the LMI (8) implies that the system is stable for all nonlinearities that satisfy the sector and slope bounds (6) and (7), respectively. Uncertainties in the parameters W_1 and W_2 in Fig. 3 can be combined with the uncertainty in the nonlinearity when applying the robust stability condition.

3.2. Performance analysis

The input w of the system described in Fig. 2(b) is assumed to belong to a set of $\mathcal{L}_2$-norm-bounded functions. Sufficient conditions for the $\mathcal{L}_2$-gain of a system in SNOF to be finite and less than some bound have been derived in terms of convex optimizations with LMI constraints (e.g. see [22,38,39] and citations therein). As for stability conditions, which performance condition to use depends on the assumptions made on the uncertainty in the nonlinearity inversion. The following sufficient condition, which is applied in the pH control case study, quantifies the performance for nonlinearities that are diagonal, static, sector-bounded, and slope-restricted.

Theorem 3 ($\mathcal{L}_2$-Gain performance condition). *Consider the system described in Fig. 2(b) with*

$$\begin{aligned} x_{k+1} &= Ax_k + B_p p_k + B_w w_k \\ q_k &= C_q x_k + D_{qp} p_k + D_{qw} w_k \\ z_k &= C_z x_k + D_{zp} p_k + D_{zw} w_k \end{aligned} \tag{9}$$

where $p_k = \Gamma(q_k)$ satisfies the sector-bounded and slope-restricted conditions (6) and (7), $A \in \mathbb{R}^{n\times n}$, $B_p \in \mathbb{R}^{n\times h}$, $B_w \in \mathbb{R}^{n\times m}$, $C_q \in \mathbb{R}^{h\times n}$, $C_z \in \mathbb{R}^{r\times n}$, $D_{qp} \in \mathbb{R}^{h\times h}$, $D_{zw} \in \mathbb{R}^{r\times m}$, $D_{qw} \in \mathbb{R}^{h\times m}$, $D_{zp} \in \mathbb{R}^{r\times h}$, n is the number of states, h is the number of nonlinearities, m is the dimension of the input vector, and r is the dimension of the output vector.

The system of the form described in Fig. 2(b) and (9) is stable and has an upper bound on the induced $\mathcal{L}_2$-norm (or $\mathcal{L}_2$-gain) η^* if the optimization problem

$$\begin{aligned} \eta^* = \; & \min_{P,Q,\Lambda,\tilde{\Lambda}} \eta \\ & \text{s.t.} \quad P,\ P_{11} = P_{11}^{\mathrm{T}} > 0,\ Q \geq 0,\ \tilde{Q} \geq 0,\ T \geq 0,\ \tilde{T} \geq 0, \\ & \quad N \geq 0,\ \overline{G} \leq 0,\ \eta > 0 \end{aligned} \tag{10}$$

has feasible solutions, where Q, $\tilde{Q}$, T, $\tilde{T}$, and N are diagonal, $\xi = \mathrm{diag}(\xi_i)$, $\mu = \mathrm{diag}(\mu_i)$, the matrix $\overline{G} = \overline{G}^{\mathrm{T}}$ is defined by

$$\overline{G} \triangleq \overline{A}_a^{\mathrm{T}} P \overline{A}_a - \overline{E}_a^{T} P \overline{E}_a + \overline{U}_1 + \overline{U}_2 - \overline{S}_1 - \overline{S}_2 - \overline{S}_3 - \begin{bmatrix} \mathbf{0} \\ \mathbf{0} \\ \mathbf{0} \\ \mathbf{I} \end{bmatrix} \begin{bmatrix} \mathbf{0} & \mathbf{0} & \mathbf{0} & \mathbf{I} \end{bmatrix}$$

$$+ \frac{1}{\eta^2} \begin{bmatrix} C_z^{\mathrm{T}} \\ D_{zp}^{\mathrm{T}} \\ \mathbf{0} \\ D_{zw}^{\mathrm{T}} \end{bmatrix} \begin{bmatrix} C_z & D_{zp} & \mathbf{0} & D_{zw} \end{bmatrix}, \tag{11}$$

and the matrices $\overline{A}_a$, $\overline{E}_a$, $\overline{U}_1$, $\overline{U}_2$, $\overline{S}_1$, $\overline{S}_2$, and $\overline{S}_3$ are defined in Appendix F.

4. Results: application to pH neutralization

Consider the continuous pH neutralization of an acid stream by a highly concentrated basic stream (see Fig. 4). The only measured signal is the controlled variable, which is the pH, and the manipulated variable is the flow rate of basic solution. The tank has a volume of 5 l, and the 0.01 M hydrochloric (HCl) and 0.1 M caustic soda (NaOH) solutions are pumped from 200-l tanks into the mixing tank. Solutions are prepared with tap water, which contains a significant amount of dissolved carbon dioxide (in the form of aqueous HCO_3^- and CO_3^{2-}). Unmeasured disturbances include the buffering species (carbonates) in the base and acid flows, nonideal mixing in the main tank, nonideal mixing in the acid and base storage tanks, and air bubbles in the tubes through which the acid and base streams flow.

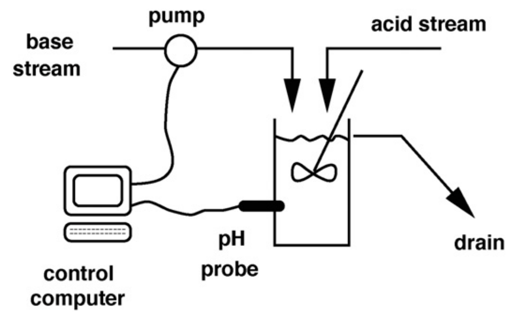

Fig. 4. pH neutralization apparatus.

In a pH process represented as a Wiener model in Fig. 1, the dynamic linear system describes the mixing dynamics and the static nonlinearity describes the titration curve [40]. Other than having a different analytical expression for the nonlinearity, the same process model was used as in [41]:

$$\begin{aligned} V\frac{dY}{dt} &= -FY - u \\ \mathrm{pH} &= W_2 \tanh(W_1 Y) \end{aligned} \tag{12}$$

where V is the volume of the mixing tank, u is the base flow rate, F is the acid flow rate, W_1 and W_2 are weights, and Y is the dimensionless strong acid equivalent [41].

For the pH process, each term in the SNOF has clear physical meaning. The nonlinearity directly corresponds to the titration curve, and the linear term directly corresponds to the mixing dynamics. Fig. 5 shows the form of the nonlinear relation between Y and pH, with some experimental data collected for a pH experimental apparatus at the University of Illinois. The process disturbances result in significant uncertainty in the nonlinearity, as shown in Fig. 5.

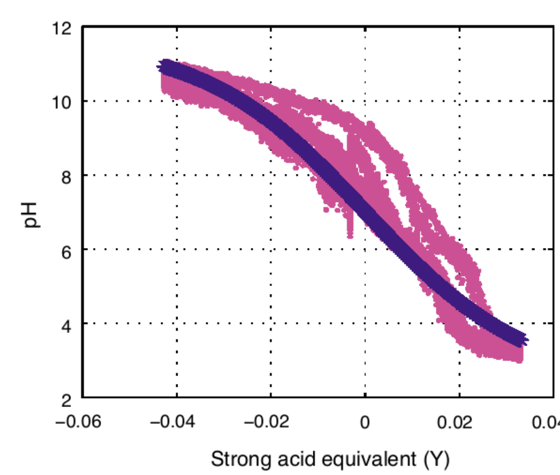

Fig. 5. Titration curve nonlinearity (W_1 and W_2 were determined by nonlinear least-squares fitting). The model is the thick blue line; experimental data points are purple dots.

Table 1
Lowest IMC filter parameter λ (in s) that indicates stability for the closed-loop system with the linear IMC controller. Perfect model information is assumed. Theorem 2 was applied with $\xi = \mu = 1$. All times are in seconds.

θ	Necessary (Theorem 1)	Sufficient (Theorem 2)
0	0.91	0.91
2	2.08	2.08
6	4.63	4.63
10	7.17	7.17
12	8.46	8.46
16	11.00	11.00

An exact discretization [32] of (12) leads to:

$$\begin{aligned} x_{k+1} &= e^{-F\Delta t/V}x_k + (1/F)(e^{-F\Delta t/V} - 1)u_k \\ Y_k &= x_k \\ \mathrm{pH}_k &= W_2\tanh(W_1 x_k) \end{aligned} \tag{13}$$

where Δt is the sampling-time. In addition, there is a time delay θ due to the sensor location. The process time delay $\theta = 0.27$ min (=16 s) and effective time constant $\tau = 3$ min were determined from experimental data by nonlinear least-squares estimation.

The linear and nonlinear IMC structures are shown in Fig. 3. The block diagram in Fig. 3 can be written directly as an SNOF.

4.1. Linear IMC design with no nonlinearity cancellation

First consider the case where the IMC is linear and the process nonlinearity Γ_1 is perfectly known and equal to tanh. Closed-loop stability results for a range of time delays are included to provide an indication as to the potential conservatism of the analysis tools for the pH neutralization problem (see Table 1). The necessary and the sufficient stability analysis results gave identical stability limits, indicating no conservatism for this closed-loop system. For this problem, the smallest stabilizing IMC filter parameter increased linearly with the time delay.

Now the linear internal model controller was designed that minimizes the desired closed-loop response time (λ) while requiring that the effect of worst-case disturbances d on the output y cannot be magnified by more than a factor of 2.5. This is a direct nonlinear generalization of the linear IMC design procedure for the specification that the peak sensitivity is less than 2.5 [26,31]. The performance measure for a range of controller tuning parameter λ for the linear IMC controller is shown in Fig. 6. The optimal λ is equal to 8.5 min. This performance condition places a much

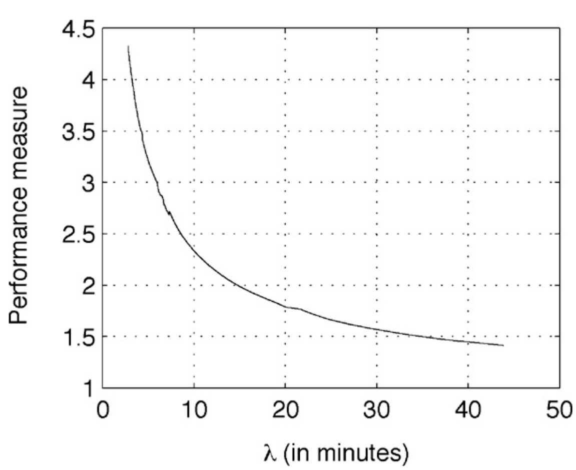

Fig. 6. Performance measure η^* for the closed-loop system with the linear internal model controller with tuning parameter λ (for a process time delay $\theta = 0.27$ min).

Table 2
Lowest IMC filter parameter λ (in seconds) that indicates robust stability for the closed loop system with the nonlinear IMC controller and significant uncertainty in the process nonlinearity.

θ	Necessary (Theorem 1)	Sufficient (Theorem 2)
0	1.44	1.44
2	3.71	4.28
6	8.79	9.38
10	13.88	14.49
12	16.44	17.04
16	21.52	22.17

stronger restriction on the closed-loop speed of response than the requirement of nominal stability.

4.2. Nonlinear IMC design with perfect nonlinearity cancellation

The geometric control literature commonly assumes that the nonlinear process is perfectly known. This assumption would imply that the controller nonlinearity Γ_2 (in Fig. 3) perfectly cancels the process nonlinearity Γ_1, and the closed-loop stability could be determined from linear stability analysis. The resulting stability conditions are exactly the same as those used to compute the necessary condition in Table 1. Hence for the pH neutralization process under the assumption of a perfect model, the stability limit for the linear IMC is equal to the stability limit for the nonlinear IMC, which is λ = 11 s for the time delay $\theta = 16$ s.

4.3. Nonlinear IMC design with robustness to uncertainty in nonlinearity inversion

Nonlinear models are rarely of very high accuracy, and this is certainly true for the pH neutralization process as demonstrated in Fig. 5. Now a nonlinear IMC controller is designed that minimizes the desired closed-loop response time (λ) while requiring stability to uncertainties in the cancellation of the process nonlinearity, which is mathematically represented as deviations in $\Gamma_2\Gamma_1$ from one. Based on close inspection of Fig. 5, it was assumed that the maximum overall slope of $\Gamma_2\Gamma_1$ could be as high as two, while its instantaneous slope could be off as much as a factor of four. Ensuring stability for this range of uncertainties is a nonlinear generalization of the common objective used in the design of controllers for linear systems of providing a gain margin of 2. Table 2 gives stability limits for a range of time delays to provide some indication of potential conservatism of the stability analysis results. The minimum IMC filter parameter λ that provides robust stability increases linearly with the time delay. The minimize filter parameter is λ ≈ 22 s for the time delay $\theta = 16$ s, which is twice the value computed for the nonlinear IMC design that ignored uncertainty in the nonlinearity inversion.

5. Discussion

Whether a performance or stability constraint was used in the IMC design had a significant influence on the filter parameter λ in the nonlinear IMC-based controller. For the pH neutralization process, controllers tuned based on a nominal stability or robust stability constraint provided much faster closed-loop speed of response than the controller based on the worst-case performance constraint. This observation indicates the importance of carefully choosing the controller design criteria.

The sufficient stability condition in Theorem 2 was nonconservative to three significant figures for the closed-loop system controlled by the linear internal model controller, for a range of time delays (see Table 1). For the stability analysis that took the uncertainty in the nonlinearity inversion into account, the

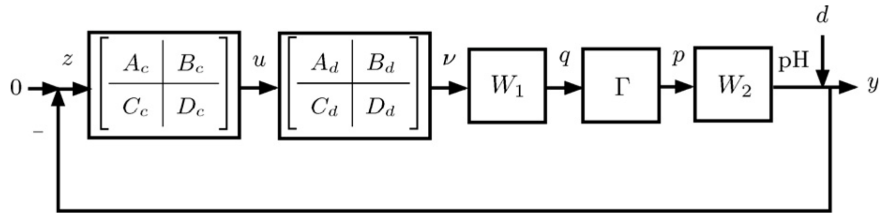

Fig. 7. Block diagram for pH system.

sufficient condition could potentially be somewhat conservative, as there is a gap in the values for the minimize allowable filter parameter λ computed from the necessary condition and sufficient conditions (see Table 2). The gap is less than 0.1% for a system with no time delay and about 3% for the time delay of 16 s identified in the experiments. The gap in the values of the minimum λ for the other time delays are all about 0.6 s (see Table 2). Although the limits computed from the necessary and the sufficient conditions are not exactly equal, they are certainly close enough for practical application.

The stability analysis that took uncertainty in the nonlinearity inversion into account indicated that the minimum stabilizing values for the filter parameter λ were twice as large as the values that were computed that ignored the uncertainty in the nonlinearity inversion. This observation indicates that importance of taking uncertainty during nonlinearity inversion into account when designed nonlinear inversion-based controllers.

The approach in this paper can be extended to nonlinear operators Γ in which each of its outputs is related to each of its inputs from conditions such as shown in Theorem 2. The simplest way to implement this generalization is to rearrange the scalar nonlinearities to form a larger diagonal nonlinear operator in Fig. 2. The expressions for the state-space matrices in Fig. 2 are messier. The generalization to full-block or block-diagonal nonlinear operators Γ follows the same derivations, but with much messier nomenclature.

The approach in this paper applies to systems with larger time delays. Appendix B shows the transformation of a system with potentially large time delay into the standard state-space system description; this transformation is standard in the control literature. The computational cost of analyzing systems with larger time delays is much smaller than suggested by the increase in dimensions, because the state-space matrices for the extended system in Appendix B are highly sparse, and many existing LMI solvers are effective at exploiting sparsity (e.g. [23,24]).

6. Conclusions

A nonlinear internal model control procedure was presented for stable Wiener systems that ensures robustness of closed-loop stability and performance to uncertainties in the inversion of the static nonlinearity, while having polynomial-time computational cost. Several more general observations can be made based on a pH control case study. Assuming perfect nonlinearity inversion when controlling pH processes led to overly optimistic predictions on the achievable closed-loop performance, which indicates that the commonly made assumption of perfect nonlinearity inversion can produce poor results in practical applications. A comparison of pH controllers designed to satisfy robust stability or disturbance suppression constraints showed that the closed-loop response speed could significantly change depending on the design criteria. A comparison of the sufficient robust stability condition with a necessary condition showed that the sufficient robust stability condition was nonconservative for this particular application.

The nonlinear IMC procedure is applicable to stable Wiener systems with unstable zero dynamics, unmeasured states, disturbances, and measurement noise. This is in contrast to many nonlinear control methods that require stable zero dynamics and/or ignore disturbances and measurement noise. The generalization of the approach to Hammerstein and Sandwich models is straightforward, and can be used to explicitly incorporate actuator constraints into the nonlinear controller design, by combining these static nonlinearities with any other static nonlinearity associated with the input to the process. The approach can also be combined with directionality compensation, which can improve the closed-loop dynamics for ill-conditioned processes [42,43].

Acknowledgments

Support is acknowledged from the Process Systems Engineering Consortium and the last author acknowledges support from the Gilliland Professorship.

Recollections of Ken Muske

Everyone in the process control community knew of Ken through his papers on model predictive control in the mid 1990s, and his presence was continuously felt through his very high degree of professional service to the community. Ken was one of a handful of process control engineers who have been very active in the organization of the American Control Conferences in the last decade, which are managed by the American Automatic Control Council (AACC) of eight societies that include the American Institute of Chemical Engineers (AIChE) and the Institute of Electrical and Electronics Engineers (IEEE). Ken's leadership that I personally had witnessed for the AACC and AIChE motivated me to nominate him for the Program Coodinator of the Systems and Process Control area of the AIChE Computing and Systems Technology (CAST) divison, as he was demonstrating a much higher degree of professional service in the field than the other U.S. process control engineer that had not yet held that position. I was pleased when Ken was selected for the position, and he continued to be selected and elected into higher leadership positions, including on the AACC Board of Directors and Director of the CAST divison of AIChE.

Mostly in service to AIChE and AACC, we simultaneously served on numerous organizing and program committees, served back-to-back terms for leadership positions, and interacted very closely. Many times we were organizing papers into sessions and scheduling sessions for American Control Conferences, debating the merits of nominations for awards, or discussing strategies for encouraging other AIChE members to become more involved in AACC activities. We also discussed control education, a subject that Ken cared deeply about, and I was looking forward to a tutorial paper that I had invited him to give at the 2010 American Control Conference.

Ken cared deeply about the control profession, always tried to do the best for the community, and always behaved with a very high degree of professional and personal ethics. I am not ashamed to admit that I cried when I learned of his passing, and I am crying as I write this sentence. I miss Ken deeply, and I always will.

-Richard D. Braatz

Appendix A. Computation of SNOF for pH system

Consider the block diagram in Fig. 7 where $\left[\begin{array}{c|c} A_d & B_d \\ \hline C_d & D_d \end{array}\right] \triangleq C_d(z\mathbf{I}-A_d)^{-1}B_d + D_d$ and $w = d$. The system equation is given by

$$
\begin{aligned}
z_k &= -(\mathrm{pH}_k + w_k) = -W_2 p_k - w_k \\
q_k &= W_1 \nu_k \\
&= W_1 (C_d Y_k + D_d C_c x_k - D_d D_c W_2 p_k - D_d D_c w_k) \\
Y_{k+1} &= A_d Y_k + B_d C_c x_k - B_d D_c W_2 p_k - B_d D_c w_k \\
x_{k+1} &= A_c x_k - B_c W_2 p_k - B_c w_k \\
p_k &= \Gamma(q_k).
\end{aligned}
$$

Define the concatenated vector $\hat{x}_k \triangleq (Y_k, x_k)^{\mathrm{T}}$, then the SNOF in Fig. 2(b) for the pH system is given by

$$
\begin{aligned}
\hat{x}_{k+1} &= \underbrace{\begin{bmatrix} A_d & B_d C_c \\ 0 & A_c \end{bmatrix}}_{A} \hat{x}_k + \underbrace{\begin{bmatrix} -B_d D_c W_2 \\ -B_c W_2 \end{bmatrix}}_{B_p} p_k + \underbrace{\begin{bmatrix} -B_d D_c \\ -B_c \end{bmatrix}}_{B_w} w_k \\
q_k &= \underbrace{\begin{bmatrix} W_1 C_d & C_1 D_d C_c \end{bmatrix}}_{C_q} \hat{x}_k + \underbrace{\begin{bmatrix} -W_1 D_d D_c W_2 \end{bmatrix}}_{D_{qp}} p_k \\
&\quad + \underbrace{\begin{bmatrix} -W_1 D_d D_c \end{bmatrix}}_{D_{qw}} w_k \\
z_k &= \underbrace{\begin{bmatrix} 0 \end{bmatrix}}_{C_z} \hat{x}_k + \underbrace{\begin{bmatrix} -W_2 \end{bmatrix}}_{D_{zp}} p_k + \underbrace{\begin{bmatrix} -\mathbf{I} \end{bmatrix}}_{D_{zw}} w_k.
\end{aligned}
$$

Appendix B. Extended state-space representation for systems with time-delay in input channels.

Consider the discrete-time system model

$$x_{k+1} = A_d(\Delta t) x_k + B_d(\Delta t) \tilde{u}_k(\theta) \tag{B.1}$$

where Δt is the sampling interval for discretization such that $x_k = x(k\Delta t)$ and $\tilde{u}_k(\theta) \triangleq u(k\Delta t - \theta)$ with time delay θ. Suppose that $\theta = m\Delta t$ where m is an integer. Then the system equation can be written as

$$x_{k+1} = A_d(\Delta t) x_k + B_d(\Delta t) u_{k-m} \tag{B.2}$$

Define the auxiliary states

$$
\begin{aligned}
\zeta^0_{k+1} &\triangleq A_d(\Delta t)\zeta^0_k + B_d(\Delta t) u_k, \\
\zeta^{\ell+1}_{k+1} &\triangleq \zeta^{\ell}_k, \quad \ell = 0, \ldots, m-1.
\end{aligned} \tag{B.3}
$$

Then the state of the system (B.1) is the output of the extended state-space model:

$$
\begin{aligned}
\zeta_{k+1} &= \mathcal{A}_d(\Delta t)\zeta_k + \mathcal{B}_d(\Delta t) u_k \\
x_k &= \mathcal{C}_d \zeta_k
\end{aligned} \tag{B.4}
$$

where $\zeta \triangleq \mathrm{vec}(\zeta^0, \zeta^1, \cdots, \zeta^m) \in \mathbb{R}^{nm}$ and[4]

$$
\mathcal{A}_d(\Delta t) \triangleq \begin{bmatrix}
A_d(\Delta t) & \mathbf{0} & \cdots & \cdots & \cdots & \mathbf{0} \\
\mathbf{I} & \mathbf{0} & \cdots & \cdots & \cdots & \mathbf{0} \\
\mathbf{0} & \mathbf{I} & \mathbf{0} & \cdots & \cdots & \mathbf{0} \\
\mathbf{0} & \mathbf{0} & \mathbf{I} & \mathbf{0} & \cdots & \mathbf{0} \\
\vdots & \vdots & \ddots & \ddots & \ddots & \mathbf{0} \\
\mathbf{0} & \mathbf{0} & \mathbf{0} & \cdots & \mathbf{I} & \mathbf{0}
\end{bmatrix}, \quad
\mathcal{B}_d(\Delta t) \triangleq \begin{bmatrix} B_d(\Delta t) \\ \mathbf{0} \\ \vdots \\ \vdots \\ \vdots \\ \mathbf{0} \end{bmatrix},
$$

$$\mathcal{C}_d \triangleq \begin{bmatrix} \mathbf{0} & \cdots & \cdots & \cdots & \mathbf{0} & \mathbf{I} \end{bmatrix}.$$

Proposition 1. *The system (B.1) is stable if and only if the system (B.4) is stable.*

Proof. ($\Leftarrow$): This direction is shown by observing that the state vector in (B.1) is a subset of the state vector in (B.4), that is, $\zeta^m = x$. ($\Rightarrow$): Suppose that the system (B.1) has a unique stable steady-state x^{eq}. Then, there exists a sufficiently large $K \in \mathbb{Z}_+$ such that $\zeta^m_k = x^{\mathrm{eq}}$ for all $k \geq K$, where it can be assumed that $K \gg m$ without loss of generality. This implies that $\zeta^{\ell}_{\kappa} = x^{\mathrm{eq}}$, $\ell = 0, \ldots, m-1$ for all $\kappa \geq K - m$, which is equivalent to stability of the system (B.4). □

Appendix C. Proof of Theorem 2

Proof. Consider the Lyapunov function

$$
\begin{aligned}
V(x_k) &= \overline{x}_k^T P \overline{x}_k + 2\sum_{i=1}^{n_q} Q_{ii} \int_0^{q_{k,i}} \phi_i(\sigma) d\sigma \\
&\quad + 2\sum_{i=1}^{n_q} \tilde{Q}_{ii} \int_0^{q_{k,i}} \left[\xi_i \sigma - \phi_i(\sigma)\right] d\sigma,
\end{aligned}
$$

where

$$
\overline{x}_k \triangleq \begin{bmatrix} x_k \\ p_k \\ q_k \end{bmatrix}, P^T = P \triangleq \begin{bmatrix} P_{11} & P_{12} & P_{13} \\ P_{12}^T & P_{22} & P_{23} \\ P_{13}^T & P_{23}^T & P_{33} \end{bmatrix} \geq 0, P_{11} > 0,
$$

$$Q_{ii} \geq 0, \tilde{Q}_{ii} \geq 0, \forall i = 1, \ldots, n_q,$$

and the subscript k indicates a sampling instance. Both p_k and q_k are functions of the state variable vector x_k, and the above Lyapunov function is radially unbounded and positive for all nonzero $x_k \in \mathbb{R}^n$. The difference in the Lyapunov function between the $k+1$ and k sampling instances is

$$
\begin{aligned}
\Delta V(x_k) &= \zeta_k^T (A_a^T P A_a - E_a^T P E_a)\zeta_k + 2\sum_{i=1}^{n_q} Q_{ii} \int_{q_{k,i}}^{q_{k+1,i}} \phi_i(\sigma) d\sigma \\
&\quad + 2\sum_{i=1}^{n_q} \tilde{Q}_{ii} \int_{q_{k,i}}^{q_{k+1,i}} \left[\xi_i \sigma - \phi_i(\sigma)\right] d\sigma,
\end{aligned} \tag{C.1}
$$

where $\zeta_k \triangleq \begin{bmatrix} x_k \\ p_k \\ p_{k+1} \end{bmatrix}$, $A_a \triangleq \begin{bmatrix} A & B & 0 \\ 0 & 0 & I \\ CA & CB & D \end{bmatrix}$, $E_a \triangleq \begin{bmatrix} I & 0 & 0 \\ 0 & I & 0 \\ C & D & 0 \end{bmatrix}$

[4] $\mathrm{vec}(a, b) \in \mathbb{R}^{n_1+n_2}$ refers to the concatenation of vectors $a \in \mathbb{R}^{n_1}$ and $b \in \mathbb{R}^{n_2}$, i.e., its first n_1 entries are equal to a and the remaining entries are equal to b

Slope restrictions on the nonlinearities place an upper bound on the first integral:

$$2\sum_{i=1}^{n_q} Q_{ii}\int_{q_{k,i}}^{q_{k+1,i}}\phi(\sigma)d\sigma \le 2\sum_{i=1}^{n_q} Q_{ii}\{(\phi_{k+1,i}-\phi_{k,i})(q_{k+1,i}-q_{k,i}) - \frac{1}{2\mu_i}(\phi_{k+1,i}-\phi_{k,i})^2\} = \zeta_k^T U_1 \zeta_k,$$

where U_1 is given in Appendix D. Similarly, an upper bound can be derived on the second integral:

$$2\sum_{i=1}^{n_q}\tilde{Q}_{ii}\int_{q_{k,i}}^{q_{k+1,i}}\left[\xi_i\sigma-\phi(\sigma)\right]d\sigma = -2\sum_{i=1}^{n_q}\tilde{Q}_{ii}\int_{q_{k,i}}^{q_{k+1,i}}\phi(\sigma)d\sigma + 2\sum_{i=1}^{n_q}\tilde{Q}_{ii}\int_{q_{k,i}}^{q_{k+1,i}}\xi_i\sigma d\sigma \le -2\sum_{i=1}^{n_q}\tilde{Q}_{ii}\left\{\frac{1}{2\mu_i}(\phi_{k+1,i}-\phi_{k,i})^2 + \phi_{k,i}(q_{k+1,i}-q_{k,i})\right\} + 2\sum_{i=1}^{n_q}\tilde{Q}_{ii}\xi_i[q_{k+1,i}^2-q_{k,i}^2] = \zeta_k^T U_2\zeta_k,$$

where U_2 is given in Appendix D.

$$\sum_{i=1}^{n_q} 2\tilde{\tau}_i\phi_{k+1,i}[\xi_i^{-1}\phi_{k+1,i}-q_{k+1,i}] = \zeta_k^T S_2\zeta_k, \tag{C.5}$$

where S_1 and S_2 are given in Appendix D. A similar notation based on the inequality (C.3) is:

$$\sum_{i=1}^{n_q} 2N_{ii}(\phi_{k+1,i}-\phi_{k,i})[\mu_i^{-1}(\phi_{k+1,i}-\phi_{k,i}) - (q_{k+1,i}-q_{k,i})] = \zeta_k^T S_3\zeta_k, \tag{C.6}$$

where S_3 is given in Appendix D.

Applying the S-procedure, if the LMI $G \triangleq A_a^T P A_a - E_a^T P E_a + U_1 + U_2 - S_1 - S_2 - S_3 < 0$ is feasible then $\Delta V(x_k) < 0$ is satisfied for the specific class of feedback-connected nonlinearities $\phi \in \Phi_{sb}^{[0,\xi]} \cap \Phi_{sr}^{[0,\mu]}$. All of introduced matrix (decision) variables are of compatible dimensions. □

Appendix D. Matrices for the application of the S-procedure in Theorem 2

$$U_1 \triangleq \begin{bmatrix} 0 & -(CA-C)^T Q & (CA-C)^T Q \\ * & -Q(CB-D)-(CB-D)^T Q - Q\mu^{-1} & -QD+Q\mu^{-1} \\ * & * & -QD-D^T Q - Q\mu^{-1}\end{bmatrix}$$

$$U_2 \triangleq \begin{bmatrix} A^T C^T\tilde{Q}\xi CA - C^T\tilde{Q}\xi C & A^T C^T\tilde{Q}\xi CB - (CA-C)^T\tilde{Q} - C^T\tilde{Q}\xi D & A^T C^T\tilde{Q}\xi D \\ * & \begin{pmatrix} B^T C^T\tilde{Q}\xi CB + D^T\tilde{Q}\xi D \\ -(CB-D)^T\tilde{Q} - \tilde{Q}(CB-D) - \mu^{-1}\tilde{Q}\end{pmatrix} & \mu^{-1}\tilde{Q} - \tilde{Q}D + B^T C^T\tilde{Q}\xi D \\ * & * & -\mu^{-1}\tilde{Q} + 2D^T\tilde{Q}\xi D\end{bmatrix}$$

$$S_1 \triangleq \begin{bmatrix} 0 & -C^T T & 0 \\ * & 2\xi^{-1}T - TD - D^T T & 0 \\ * & * & 0\end{bmatrix}, \quad S_2 \triangleq \begin{bmatrix} 0 & 0 & -A^T C^T\tilde{T} \\ * & 0 & -B^T C^T\tilde{T} \\ * & * & 2\xi^{-1}\tilde{T} - \tilde{T}D - D^T\tilde{T}\end{bmatrix}$$

$$S_3 \triangleq \begin{bmatrix} 0 & -(CA-C)^T N & (CA-C)^T N \\ * & 2N\mu^{-1} + (CB-D)^T N + N(CB-D) & -2N\mu^{-1} + (CB-D)^T N + ND \\ * & * & 2N\mu^{-1} - D^T N - ND\end{bmatrix}.$$

Since the (negative) feedback-connected nonlinearity is monotonic with slope restriction in addition to being [0, ξ] sector-bounded, i.e., $\phi \in \Phi_{sb}^{[0,\xi]} \cap \Phi_{sr}^{[0,\mu]}$, it can be shown that the following inequalities are satisfied at each sampling instance k and all indices $i = 1, \ldots, n_q$:

$$\phi_{k,i}[\xi_i^{-1}\phi_{k,i} - q_{k,i}] \le 0, \tag{C.2}$$

$$(\phi_{k+1,i}-\phi_{k,i})[\mu_i^{-1}(\phi_{k+1,i}-\phi_{k,i}) - (q_{k+1,i}-q_{k,i})] \le 0. \tag{C.3}$$

The following notations based on (C.2) are useful when applying the S-procedure:

$$\sum_{i=1}^{n_q} 2\tau_i\phi_{k,i}[\xi_i^{-1}\phi_{k,i} - q_{k,i}] = \zeta_k^T S_1\zeta_k, \tag{C.4}$$

Appendix E. Proof of Theorem 3

Proof. It is not difficult to see that the system given in (9) is g.a.s. and is dissipative with respect to the supply rate $s(w_k, z_k) \triangleq \begin{bmatrix} w_k \\ z_k\end{bmatrix}^T \begin{bmatrix} \mathbf{I} & \mathbf{0} \\ \mathbf{0} & -\frac{1}{\eta^2}\mathbf{I}\end{bmatrix}\begin{bmatrix} w_k \\ z_k\end{bmatrix}$ and the Lyapunov function $V(x_k)$ if and only if $\Delta V(x_k) \le s(w_k, x_k)$ holds for all $k \in \mathbb{Z}$, which is equivalent to the $\mathcal{L}_2$-gain performance bound, $\sup_{\|w\|_2\le 1}\|z\|_2 \le \eta$. Consider the Lyapunov function (C.1) and the system equation (9). Then the condition $\Delta V(x_k) - s(w_k, z_k) \le 0$ can be rewritten as $\bar{\zeta}_k^T\overline{G}\bar{\zeta}_k$ where $\overline{G}$ is given in (11) and $\bar{\zeta}^T \triangleq \begin{bmatrix} x_k^T & p_k^T & p_{k+1}^T & w_k^T\end{bmatrix}$. The computation of the matrix $\overline{G}$ can be performed by using the S-procedure and the derivation is similar to the proof of Theorem 2 given in Appendix D. □

Appendix F. Matrices in Theorem 3

$$\bar{A}_a \triangleq \begin{bmatrix} A & B_p & \mathbf{0} & B_w \\ \mathbf{0} & \mathbf{0} & \mathbf{I} & \mathbf{0} \\ C_qA & C_qB_p & D_{qp} & CB_w \end{bmatrix}, \quad \bar{E}_a \triangleq \begin{bmatrix} \mathbf{I} & \mathbf{0} & \mathbf{0} & \mathbf{0} \\ \mathbf{0} & \mathbf{I} & \mathbf{0} & \mathbf{0} \\ C_q & D_{qp} & \mathbf{0} & \mathbf{0} \end{bmatrix},$$

$$\bar{U}_1 \triangleq \begin{bmatrix} 0 & -(C_qA-C_q)^{\mathrm{T}}Q & (C_qA-C_q)^{\mathrm{T}}Q & \mathbf{0} \\ * & \begin{pmatrix} -Q(C_qB_p-D_{qp}) \\ -(C_qB_p-D_{qp})^{\mathrm{T}}Q \\ -Q\mu^{-1} \end{pmatrix} & \begin{pmatrix} (C_qB_p-D_{qp})^{\mathrm{T}}Q \\ -QD_{qp}+Q\mu^{-1} \end{pmatrix} & -QC_qB_w \\ * & * & \begin{pmatrix} Q(C_qB_p-D_{qp}) \\ +(C_qB_p-D_{qp})^{\mathrm{T}}Q \\ -Q\mu^{-1} \end{pmatrix} & QC_qB_w \\ * & * & * & \mathbf{0} \end{bmatrix},$$

$$\bar{U}_2 \triangleq \begin{bmatrix} \begin{pmatrix} A^{\mathrm{T}}C_q^{\mathrm{T}}\xi\tilde{Q}C_qA \\ -C_q^{\mathrm{T}}\xi\tilde{Q}C_q \end{pmatrix} & \begin{pmatrix} (C_qA-C_q)^{\mathrm{T}}\xi \\ \cdot\tilde{Q}(C_qB_p+D_{qp}) \\ -(C_qA-C_q)^{\mathrm{T}}\tilde{Q} \end{pmatrix} & \begin{pmatrix} (C_qA-C_q)^{\mathrm{T}} \\ \cdot\xi\tilde{Q}D_{qp} \end{pmatrix} & \begin{pmatrix} (C_qA-C_q)^{\mathrm{T}} \\ \cdot\xi\tilde{Q}C_qB_w \end{pmatrix} \\ * & \begin{pmatrix} 2(C_qB_p+D_{qp})^{\mathrm{T}}\xi \\ \cdot\tilde{Q}(C_qB_p+D_{qp}) \\ -\tilde{Q}(C_qB_p-D_{qp}) \\ -(C_qB_p-D_{qp})^{\mathrm{T}}\tilde{Q} \\ -\tilde{Q}\mu^{-1} \end{pmatrix} & \begin{pmatrix} (C_qB_p+D_{qp})^{\mathrm{T}} \\ \cdot\xi\tilde{Q}D_{qp} \\ -\tilde{Q}D_{qp}+\tilde{Q}\mu^{-1} \end{pmatrix} & \begin{pmatrix} (C_qB_p+D_{qp})^{\mathrm{T}} \\ \cdot\xi\tilde{Q}C_qB_w \\ -\tilde{Q}C_qB_w \end{pmatrix} \\ * & * & 2D_{qp}\xi\tilde{Q}D_{qp}-\tilde{Q}\mu^{-1} & D_{qp}^{\mathrm{T}}\xi\tilde{Q}C_qB_w \\ * & * & * & 2B_w^{\mathrm{T}}C_q^{\mathrm{T}}\xi\tilde{Q}C_qB_w \end{bmatrix},$$

$$\bar{S}_1 \triangleq \begin{bmatrix} \mathbf{0} & -C_q^{\mathrm{T}}T & \mathbf{0} & \mathbf{0} \\ * & 2\xi^{-1}T-TD_{qp}-D_{qp}^{\mathrm{T}}T & \mathbf{0} & \mathbf{0} \\ * & * & \mathbf{0} & \mathbf{0} \\ * & * & * & \mathbf{0} \end{bmatrix}, \bar{S}_2 \triangleq \begin{bmatrix} 0 & -A^{\mathrm{T}}C_q^{\mathrm{T}}\tilde{T} & \mathbf{0} & \mathbf{0} \\ * & -B_q^{\mathrm{T}}C_q^{\mathrm{T}}\tilde{T}-\tilde{T}C_qB_p & -\tilde{T}D_{qp} & \tilde{T}C_qB_w \\ * & * & 2\xi^{-1}\tilde{T} & \mathbf{0} \\ * & * & * & -B_q^{\mathrm{T}}C_q^{\mathrm{T}}\tilde{T} \end{bmatrix},$$

$$\bar{S}_3 \triangleq \begin{bmatrix} 0 & -(C_qA-C_q)^{\mathrm{T}}N & \mathbf{0} & \mathbf{0} \\ * & \begin{pmatrix} (C_qB_p-D_{qp})^{\mathrm{T}}N \\ +N(C_qB_p-D_{qp}) \\ +2N\mu^{-1} \end{pmatrix} & \begin{pmatrix} (C_qB_p-D_{qp})^{\mathrm{T}}N \\ -2N\mu^{-1}+ND_{qp} \end{pmatrix} & NC_qB_w \\ * & * & 2N\mu^{-1}-D_{qp}^{\mathrm{T}}N-ND_{qp} & -NC_qB_w \\ * & * & * & \mathbf{0} \end{bmatrix}.$$

References

[1] E. Eskinat, S.H. Johnson, W.L. Luyben, Use of Hammerstein models in identification of nonlinear-systems, AIChE J. 37 (1991) 255–268.

[2] J.C. Gomez, E. Baeyens, Identification of block-oriented nonlinear systems using orthonormal bases, J. Process Control 14 (2004) 685–697.

[3] F.J. Doyle III,;1; Robustness properties of nonlinear process control and implications for the design and control of a packed reactor, PhD thesis, California Institute of Technology, Pasadena, CA, 1991.

[4] J.G. VanAntwerp, R.D. Braatz, N.V. Sahinidis, Robust nonlinear control of plasma etching, in: Proc. Electrochem. Soc., 1997, pp. 454–462.

[5] J.G. VanAntwerp, R.D. Braatz, N.V. Sahinidis, Globally optimal robust process control, J. Process Control 9 (1999) 374–383.

[6] G. Pajunen, Adaptive control of Wiener type nonlinear systems, Automatica 28 (1992) 781–785.

[7] A. Kalafatis, L. Wang, W.R. Cluett, Linearizing feedforward-feedback control of pH processes based on the Wiener model, J. Process Control 15 (2005) 103–112.

[8] R.S. Patwardhan, S. Lakshminarayanan, S.L. Shah, Constrained nonlinear MPC using Hammerstein and Wiener models: PLS framework, AIChE J. 44 (1998) 1611–1622.

[9] S.J. Norquay, A. Palazoglu, J.A. Romagnoli, Application of Wiener model predictive control (wmpc) to a pH neutralization experiment, IEEE Trans. Control Sys. Technol. 7 (1999) 437–445.

[10] O. Toker, H. Ozbay, On the NP-hardness of solving bilinear matrix inequalities and simultaneous stabilization with static output feedback, in: Proc. of American Control Conference, Seattle, WA, USA, 1995, pp. 2525–2526.

[11] F.G. Shinskey, pH and pION Control in Process and Waste Streams, Wiley, New York, 1973.

[12] A. Johnson, The control of fed-batch fermentation processes-A survey, Automatica 23 (1987) 691–705.

[13] R.A. Wright, C. Kravaris, On-line identification and nonlinear control of an industrial pH process, J. Process Control 11 (2001) 361–374.

[14] A. Faanes, S. Skogestad, pH-neutralization: Integrated process and control design, Comput. Chem. Eng. 28 (2004) 1475–1487.

[15] J. Barraud, Y. Creff, N. Petit, pH control of a fed batch reactor with precipitation, J. Process Control 19 (2009) 888–895.

[16] I.A. Lur'e, V.N. Postnikov, On the theory of stability of control systems, Appl. Math. Mech. 8 (1944) 246–248.

[17] A.L. Fradkov, V.A. Yakubovich, The S-procedure and a duality relations in nonconvex problems of quadratic programming, Vestnik Leningrad Univ. Math. 5 (1973) 101–109.
[18] A. Megretski, S. Treil, Power distribution inequalities in optimization and robustness of uncertain systems, J. Math. Sys. Est. Control 3 (1993) 301–319.
[19] K. Kim, R.D. Braatz, Universal approximation with error bounds for dynamic artificial neural network models: A tutorial and some new results, in: Proc. of the IEEE Multi-Conference on Systems and Control, IEEE Press, Piscataway, NJ, 2011, pp. 834–839.
[20] K. Kim, R.D. Braatz, Standard representation and stability analysis of dynamic artificial neural networks: A unified approach, in: Proc. of the IEEE Multi-Conference on Systems and Control, IEEE Press, Piscataway, NJ, 2011, pp. 840–845.
[21] K. Kim, Robust control for systems with sector-bounded, slope-restricted, and odd monotonic nonlinearities using linear matrix inequalities, Master's thesis, University of Illinois at Urbana-Champaign, Illinois, USA, 2009.
[22] S. Boyd, L. El Ghaoui, E. Feron, V. Balakrishnan, Linear Matrix Inequalities in System and Control Theory, SIAM, Philadelphia, 1994.
[23] J.F. Sturm, Using SeDuMi 1.02, A MATLAB toolbox for optimization over symmetric cones, Optim. Methods Softw. 11-12 (1998) 625–653.
[24] J. Löfberg, YALMIP: A toolbox for modeling and optimization in MATLAB, in: Proc. Computer-Aided Control System Design Conf. (2004), IEEE Press, Piscataway, NJ, 2004, pp. 284–289.
[25] Z. Szabo, P. Gaspar, J. Bokor, Reference tracking for Wiener systems using dynamic inversion, in: Proc. of the Joint Conf. of the 20th IEEE International Symposium on Intelligent Contol and 13th Mediterranean Conf. on Control and Automation, 2005, pp. 1196–1200.
[26] M. Morari, E. Zafiriou, Robust Process Control, Prentice-Hall, Englewood Cliffs, NJ, 1989.
[27] K. Zhou, J.C. Doyle, Essentials of Robust Control, Prentice-Hall, Upper Saddle River, NJ, 1998.
[28] T. Basar, P. Bernhard, H_∞-Optimal Control and Related Minimax Design Problems: A Dynamic Game Approach, 2nd ed., Birkhauser, Boston, 1995.
[29] R.D. Braatz, P.M. Young, J.C. Doyle, M. Morari, Computational complexity of μ-calculation, IEEE Trans. Automatic Control 39 (1994) 1000–1002.
[30] M. Kishida, R.D. Braatz, Internal model control, in: W.S. Levine (Ed.), The Control Handbook, 2nd ed., CRC Press, Boca Raton, Florida, 2011, pp. 9:100–123.
[31] S. Skogestad, I. Postlethwaite, Multivariable Feedback Control: Analysis and Design, John Wiley & Sons, New York, 1996.
[32] T. Chen, B.A. Francis, Optimal Sampled-data Control Systems, Springer, New York, 1995.
[33] I.G. Horn, J.R. Arulandu, C.J. Gombas, J.G. VanAntwerp, R.D. Braatz, Improved filter design in internal model control, Ind. Eng. Chem. Res. 35 (1996) 3437–3441.
[34] B.W. Bequette, Process Control: Modeling, Design and Simulation, Prentice-Hall, Upper Saddle River, NJ, 2003.
[35] C.G. Economou, M. Morari, B.O. Palsson, Internal model control: Extension to nonlinear system, Ind. Eng. Chem. Process Des. Dev. 25 (1986) 403–411.
[36] M.A. Henson, D.E. Seborg, An internal model control strategy for nonlinear systems, AIChE J. 37 (1991) 1065–1081.
[37] H.K. Khalil, Nonlinear Systems, Prentice Hall, Upper Saddle River, NJ, 2002.
[38] A.N. Michel, D. Liu, Qualitative Analysis and Synthesis of Recurrent Neural Networks, Marcel Dekker, New York, 2002.
[39] J.G. VanAntwerp, R.D. Braatz, A tutorial on linear and bilinear matrix inequalities, J. Process Control 10 (2000) 363–385.
[40] A. Kalafatis, N. Arifin, L. Wang, W.R. Cluett, A new approach to identification of pH processes based on the Wiener model, Chem. Eng. Sci. 50 (1995) 3693–3701.
[41] B. Ogunnaike, R.A. Wright, Industrial applications of nonlinear control, in: Fifth Int. Conf. on Chemical Process Control, 1997, pp. 46–59.
[42] P.J. Campo, M. Morari, Robust control of processes subject to saturation nonlinearities, Comp. Chem. Eng. 14 (1990) 343–358.
[43] M. Soroush, K.R. Muske, Analytical model predictive control, in: F. Allgower, A. Zheng (Eds.), Nonlinear Model Predictive Control, Springer, Upper Saddle River, NJ, 2000, pp. 163–179.